Thermo-optic coefficient measurement of liquids based on simultaneous temperature and refractive index sensing capability of a two-mode fiber interferometric probe

Young Ho Kim, Seong Jun Park, Sie-Wook Jeon, Seongmin Ju, Chang-Soo Park, Won-Taek Han, and Byeong Ha Lee*

School of Information and Communications, Gwangju Institute of Science and Technology, 123 Cheomdan-gwagiro, Buk-gu, Gwangju, 500-712, South Korea
**leebh@gist.ac.kr*

Abstract: A fiber-optic interferometric probe based on a two-mode fiber (TMF) is proposed and demonstrated for measuring the thermo-optic coefficients (TOCs) of liquid samples. The proposed probe can be simply fabricated by fusion-splicing a short piece of TMF to a lead single mode fiber (SMF) with small lateral offset, which makes interference between LP_{01} and LP_{02} modes. The sensing responses of the probe to temperature and surrounding refractive index (SRI) have been experimentally investigated to show the capability of simultaneous measurements; the phase change of the reflection spectrum was related to temperature variation and the intensity change was to SRI variation. The data analysis is made not only in the spectral domain but in the Fourier domain also to effectively quantify the measurements. The TOCs of several liquid samples including water, ethanol, and acetone have been obtained with the proposed method.

OCIS codes: (060.2340) Fiber optic components; (060.2370) Fiber optic sensors

References and links

1. A. Kumar, R. Jindal, R. K. Varshney, and S. K. Sharma, "A fiber-optic temperature sensor based on LP_{01}-LP_{02} mode interference," Opt. Fiber Technol. **6**(1), 83–90 (2000).
2. J. S. Sirkis, D. D. Brennan, M. A. Putman, T. A. Berkoff, A. D. Kersey, and E. J. Friebele, "In-line fiber etalon for strain measurement," Opt. Lett. **18**(22), 1973–1975 (1993).
3. X. Wang, J. Xu, Y. Zhu, K. L. Cooper, and A. Wang, "All-fused-silica miniature optical fiber tip pressure sensor," Opt. Lett. **31**(7), 885–887 (2006).
4. J. R. Zhao, X. G. Huang, W. X. He, and J. H. Chen, "High-resolution and temperature-insensitive fiber optic refractive index sensor base on Fresnel reflection modulated by Fabry-Perot interference," J. Lightwave Technol. **28**(19), 2799–2803 (2010).
5. J. Y. Cho, J. H. Lim, and K. H. Lee; "Optical fiber twist sensor with two orthogonally oriented mechanically induced long-period grating sections," IEEE Photon. Technol. Lett. **17**(2), 453–455 (2005).
6. B. H. Lee, Y. H. Kim, K. S. Park, J. B. Eom, M. J. Kim, B. S. Rho, and H. Y. Choi, "Interferometric fiber optic sensors," Sensors (Basel Switzerland) **12**(3), 2467–2486 (2012).
7. M. J. Kim, Y. H. Kim, G. Mudhana, and B. H. Lee, "Simultaneous measurement of temperature and strain based on double cladding fiber interferometer assisted by fiber grating pair," IEEE Photon. Technol. Lett. **20**(15), 1290–1292 (2008).
8. A. van Brakel and P. L. Swart, "Temperature-compensated optical fiber Michelson refractometer," Opt. Eng. **44**(2), 020504 (2005).
9. M. N. Ng, Z. Chen, and K. S. Chiang, "Temperature compensation of long-period fiber grating for refractive-index sensing with bending effect," IEEE Photon. Technol. Lett. **14**(3), 361–362 (2002).
10. H. Y. Choi, G. Mudhana, K. S. Park, U. C. Paek, and B. H. Lee, "Cross-talk free and ultra-compact fiber optic sensor for simultaneous measurement of temperature and refractive index," Opt. Express **18**(1), 141–149 (2010).
11. O. Frazao, J. L. Santos, and J. M. Baptista, "Strain and temperature discrimination using concatenated high-birefringence fiber loop mirrors," IEEE Photon. Technol. Lett. **19**(16), 1260–1262 (2007).

#174874 - $15.00 USD Received 23 Aug 2012; revised 24 Sep 2012; accepted 24 Sep 2012; published 2 Oct 2012

12. C. L. Zhao, X. Yang, and M. S. Demokan, "Simultaneous temperature and refractive index measurement using 3° slanted multimode fiber Bragg grating," J. Lightwave Technol. **24**(2), 879–883 (2006).
13. A. Iadicicco, S. Campopiano, A. Cutolo, M. Giordano, and A. Cusano, "Nonuniform thinned fiber Bragg gratings for simultaneous refractive index and temperature measurements," IEEE Photon. Technol. Lett. **17**(7), 1495–1497 (2005).
14. T. Zhu, Y. J. Rao, and Q. J. Mo, "Simultaneous measurement of refractive index and temperature using a single ultralong-period fiber grating," IEEE Photon. Technol. Lett. **17**(12), 2700–2702 (2005).
15. D. A. C. Enríquez, A. R. da Cruz, and M. T. M. R. Giraldi, "Hybrid FBG–LPG sensor for surrounding refractive index and temperature simultaneous discrimination," Opt. Laser Technol. **44**(4), 981–986 (2012).
16. S. M. Lee, S. S. Saini, and M. Y. Jeong, "Simultaneous measurement of refractive index, temperature, and strain using etched-core fiber Bragg grating sensors," IEEE Photon. Technol. Lett. **22**(19), 1431–1433 (2010).
17. X. Chen, K. Zhou, L. Zhang, and I. Bennion, "Simultaneous measurement of temperature and external refractive index by use of a hybrid grating in D fiber with enhanced sensitivity by HF etching," Appl. Opt. **44**(2), 178–182 (2005).
18. P. Lu, L. Men, K. Sooley, and Q. Chen, "Tapered fiber Mach-Zehnder interferometer for simultaneous measurement of refractive index and temperature," Appl. Phys. Lett. **94**(13), 131110 (2009).
19. S. Yaltkaya and R. Aydin, "Experimental investigation of temperature effect on the refractive index of dye laser liquids," Turk. J. Phys. **26**, 41–47 (2002).
20. J. Jasny, B. Nickel, and P. Borowicz, "Wavelength- and temperature-dependent measurement of refractive indices," J. Opt. Soc. Am. B **21**(4), 729–738 (2004).
21. S. D. Nicola, P. Mormile, and G. Pierattini, "The temperature dependence of refractive index of an aqueous suspension of polystyrene microspheres," Appl. Phys. B **53**(5-6), 350–352 (1991).
22. A. M. Vengsarkar and K. L. Walker, "Article comprising a dispersion-compensating optical waveguide," U.S. patent 5,448,674 (1995).
23. S. W. Jeon, T. Y. Kim, W. B. Kwon, and C. S. Park, "All-optical clock extraction from 10-Gbit/s NRZ-DPSK data using modal interference in a two-mode fiber," Opt. Commun. **283**(4), 522–527 (2010).
24. S. Ramachandran, S. Ghalmi, J. W. Nicholson, M. F. Yan, P. Wisk, E. Monberg, and F. V. Dimarcello, "Anomalous dispersion in a solid, silica-based fiber," Opt. Lett. **31**(17), 2532–2534 (2006).
25. S. Choi and K. Oh, "A new LP_{02} mode dispersion compensation scheme based on mode converter using hollow optical fiber," Opt. Commun. **222**(1-6), 213–219 (2003).
26. G. Lin and X. Dong, "Design of broadband $LP_{01}\leftrightarrow LP_{02}$ mode converter based on special dual-core fiber for dispersion compensation," Appl. Opt. **51**(19), 4388–4393 (2012).
27. T. Yokokawa, T. Kato, T. Fujii, Y. Yamamoto, N. Honma, A. Kataoka, M. Onishi, E. Sasaoka, and K. Okamoto, "Dispersion compensating fiber with large negative dispersion around –300 ps/km/nm and its application to compact module for dispersion adjustment," Optical Fiber Communications Conference 2003 **2**, 717–718 (2003).
28. F. D. Nunes, C. A. de Souza Melo, and H. F. da Silva Filho, "Theoretical study of coaxial fibers," Appl. Opt. **35**(3), 388–399 (1996).
29. H. Y. Choi, M. J. Kim, and B. H. Lee, "All-fiber Mach-Zehnder type interferometers formed in photonic crystal fiber," Opt. Express **15**(9), 5711–5720 (2007).
30. J. Villatoro, V. Finazzi, V. P. Minkovich, V. Pruneri, and G. Badenes, "Temperature-insensitive photonic crystal fiber interferometer for absolute strain sensing," Appl. Phys. Lett. **91**(9), 091109 (2007).
31. R. C. Kamikawachi, I. Abe, A. S. Paterno, H. J. Kalinowski, M. Muller, J. L. Pinto, and J. L. Fabris, "Determination of thermo-optic coefficient in liquids with fiber Bragg grating refractometer," Opt. Commun. **281**(4), 621–625 (2008).
32. A. H. Harveym, J. J. S. Gallagher, and M. H. L. Sengers, "Revised formulation for the refractive index of water and steam as a function of wavelength, temperature and density," J. Phys. Chem. Ref. Data **27**(4), 761–774 (1998).
33. D. Solimini, "Loss measurement of organic materials at 6328 Å," J. Appl. Phys. **37**(8), 3314–3315 (1966).

1. Introduction

For the last several decades fiber-optic sensors have been intensively investigated to measure a wide range of parameters such as temperature, strain, pressure, surrounding refractive index (SRI), twist, and so on [1–5]. As well known, fiber-optic sensors have advantages of small size, high resolution, simple fabrication, and immunity to electromagnetic interference. Especially, by introducing interferometric techniques to the fiber-optic sensors, the sensing performances have been improved in sensitivity, stability, and accuracy [6]. Importantly, the capability of multi-parameter sensing can be considered as one of the most outstanding advantages. In fact, the interference signals obtained from real experiments look more complicated when several parameters are involved at a time. It means finding the contribution of each measurand to the measured signal is necessary. Accordingly, the main issue for multi-

#174874 - $15.00 USD Received 23 Aug 2012; revised 24 Sep 2012; accepted 24 Sep 2012; published 2 Oct 2012

parameter sensing is how to discriminate each measurand when two or more perturbations are applied simultaneously. However, unfortunately, it is not simple due to the cross-sensitivity among measurands [7].

So far, many fiber-optic interferometers have been introduced to realize the multi-parameter sensing capability through overcoming the cross-sensitivity [8–18]. It can be carried out by two representative methods; one is to compensate one effect from the total measurement [8, 9] and the other is to eliminate or minimize the cross-sensitivity itself [10, 11]. The latter can be regarded as a more effective and fundamental way to solve the cross-sensitivity problem. Meanwhile, among the existing sensing modalities dealing with cross-sensitivity, the simultaneous measurements of temperature and refractive index (RI) are considered as being rather meaningful to investigate optical and chemical properties of liquid samples because the RI is strongly dependent on temperature in many cases. Such a thermal dependency of the RI is called the thermo-optic effect. The related thermo-optic coefficient (TOC) is defined as the changing rate of RI with respect to temperature variation ($\Delta n/\Delta T$) at the operating wavelength. Hence, the simultaneous monitoring of both temperature and RI variations enables to get the TOCs of specimens conveniently. Lots of works based on fiber Bragg gratings (FBGs) and long period fiber gratings (LPGs) have been reported, however, most of them required complex compensation processes to solve the inherent cross-sensitivity problem [12–17]. Furthermore, expensive fiber grating fabrication equipment limited their practical applications. Some approaches using tapering or etching have been also introduced but still had some problems including fragility and instability [16–18]. In our previous work, we have reported a dual-cavity Fabry-Perot fiber sensor to show the capability of simultaneous temperature and RI measurements [10]. However, inserting cavities and controlling their lengths were not so easy that a precise fiber control system was required. Regardless of many efforts for the simultaneous measurements, most of the works are complacent in presenting sensing performance for each measurand but rarely lead to an actual application to the TOC measurements [10, 12–18]. Rather complicated optical systems using dye laser, prism, bulk optic interferometer, and external temperature monitoring devices have been also reported [19–21].

In this paper, a simple fiber-optic probe is presented for effectively measuring the TOCs of liquid solutions. A special two-mode fiber (TMF), which can deliver only two modes (LP_{01}, LP_{02}) along the fiber, is used to form a fiber-based in-line Michelson interferometer [22]. Only one fusion-splicing between a conventional single mode fiber (SMF) and a piece of TMF is involved for the fabrication. Due to the modal dispersion of the TMF, a highly sinusoidal reflection spectrum can be obtained. The simultaneous temperature and RI sensing performances of the proposed probe are investigated and analyzed for an application to the TOC measurement. Finally, the TOCs of several liquid solutions are experimentally measured by monitoring only the spectrum variations responding to both the temperature and the RI.

2. Fabrication and operation of the TMF interferometer

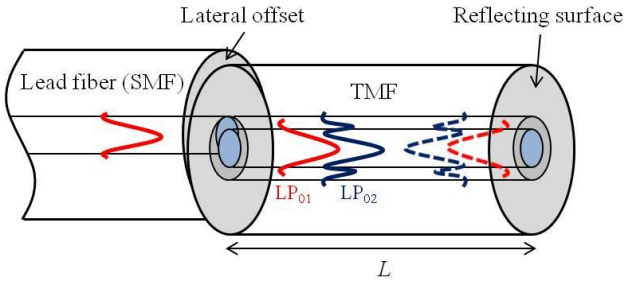

Fig. 1. Structure of the proposed TMF probe; Mode coupling arises at the offset region. The coupled two modes (LP_{01} (red) and LP_{02} (blue)) in TMF are reflected at the end surface of the TMF and finally combined into the core mode of the SMF. *L* is the TMF length.

#174874 - $15.00 USD Received 23 Aug 2012; revised 24 Sep 2012; accepted 24 Sep 2012; published 2 Oct 2012

The TMF probe was fabricated by splicing a TMF segment with a lead fiber (SMF) using a commercial fusion splicer (S183PM, FITEL Co.). First, the TMF segment was cleaved at both end faces to have a predetermined length. Then, the TMF segment was fusion spliced to the lead fiber with a small lateral offset as shown in Fig. 1. Such an intentional lateral offset is expected to give effective mode coupling in the TMF region. The amount of offset mainly affects the insertion loss and the fringe contrast of the interferometer. In experiments, the offset was applied manually and an optimum length of offset was obtained as 4 μm. Due to the unique RI profile of the TMF, it can transmit only the fundamental core mode (LP_{01}) and just one more high-order mode (LP_{02}) at the interesting wavelength range [22–26].

The light launched into the lead fiber is coupled partially to the two guided modes (LP_{01}, LP_{02}) of the TMF at the splicing region as described in Fig. 1. These two modes are Fresnel-reflected at the end surface of the TMF and re-coupled into the core mode of the SMF. Here, interference arises due to the accumulated optical path length difference (OPD) between the modes during their journey. In some previous researches, to make light coupling into the LP_{02}, some additional devices such as LPGs [24], hollow optical fibers [25], and dual-core fibers [26] have been utilized.

The TMF had a three-layered RI profile, which was designed for compensating the fiber chromatic dispersion at the 1550 nm band (DC-1429AA-1-2, Sumitomo Electric Industries) [27]. Figure 2(a) shows the RI profile of the TMF that was obtained from fiber reflectance measurement at 633 nm along the radial direction with a scanning step of 1 μm. Such a fiber structure has unique property of transmitting the LP_{01} mode through the central high index region as well as the LP_{02} mode through the ring-shaped mound [22]. In order to confirm the excitation of the LP_{02} mode as the second guided mode without exciting the LP_{11} mode in the TMF, the effective indices of both modes were calculated in terms of wavelength around the 1550 nm region by using the coaxial fiber theory [28]. As shown in Fig. 2(b), the effective index of the LP_{02} mode was slightly higher than that of the LP_{11} mode, which is different from the cases of general multimode fibers. Thus, we can say that the two guided modes of the TMF are LP_{01} and LP_{02}. As another evidence of the existing LP_{02} mode, the near field image of the coupled modes, captured by an infra-red camera at 1550 nm, is shown in the inset of Fig. 1(a). One concentric circle around the central core mode verifies that the LP_{02} mode was excited successfully with the lateral offset method.

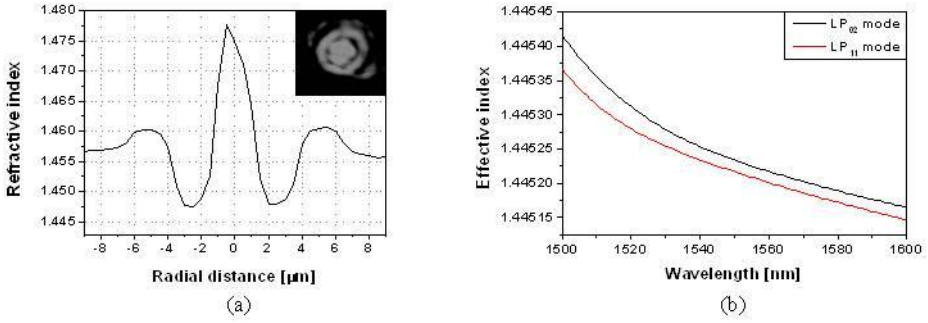

Fig. 2. (a) Refractive index profile of the TMF along the radial direction and (b) the effective indices of LP_{02} and LP_{11} modes calculated in terms of wavelength. The inset of (a) is a near field image of the coupled modes, which is captured with an infra-red camera at 1550 nm.

The intensity of the reflection spectrum $I_{out}(\lambda)$ of an ideal TMF interferometer is theoretically expressed as [29]

$$I_{out}(\lambda) = R^2(n_{sur}) \cdot \left| E_{in}(\lambda) \cdot [1 + \exp(i\phi)] \right|^2 \quad (1)$$

#174874 - $15.00 USD Received 23 Aug 2012; revised 24 Sep 2012; accepted 24 Sep 2012; published 2 Oct 2012

where R is the amplitude reflection coefficient at the TMF end face, which is given as a function of SRI n_{sur}, and $E_{in}(\lambda)$ is the amplitude spectrum of the incident light. The phase term ϕ is a function of wavelength λ in general, thus can be Taylor-expanded at the center wavelength λ_0 with the first order approximation as

$$\phi = \frac{2\pi}{\lambda}\Delta z\,(T) \approx \frac{2\pi}{\lambda_0}\left[1-\frac{\Delta\lambda}{\lambda_0}\right]\Delta z\,(T) \tag{2}$$

where $\Delta\lambda$ denotes the wavelength deviation ($\Delta\lambda = \lambda-\lambda_0$). However, the first order Taylor expansion is valid only for small $\Delta\lambda$, which mainly affect and deteriorate the linearity of the measurement.

The thermally dependent round-trip OPD $\Delta z(T)$ and its thermal variation are given by

$$\begin{aligned} &\Delta z\,(T) = \Delta n_{eff}\,(T)\cdot 2L(T),\\ &\frac{d\,\Delta z}{dT} = 2\left(\frac{d\,\Delta n_{eff}}{dT}\cdot L + \frac{dL}{dT}\cdot\Delta n_{eff}\right) = \Delta z\,(\alpha+\beta) \end{aligned} \tag{3}$$

where $\Delta n_{eff}(T)$ is the effective index difference between LP_{01} and LP_{02} modes, L is the length of the TMF segment, α is the thermal expansion coefficient of the fiber that is defined as $(1/L)dL/dT$, and β is the normalized thermo-optic coefficient of the modal index difference defined as $(1/\Delta n_{eff})d\Delta n_{eff}/dT$ [30]. Assuming practical TMF values as $\Delta n_{eff} \approx 2\text{x}10^{-2}$ and $L\approx 10^{-2}$, Δz is in the order of $4\text{x}10^{-4}$. Also, assuming 2π phase shift induced by temperature variations, $d\Delta z/dT$ is in the order of wavelength, thus, $1.55\text{x}10^{-6}$. When we consider those assumptions, $\alpha+\beta$ should be in the order of $3.88\text{x}10^{-3}$. Since the reported value of α for pure silica is about $5\text{x}10^{-7}$ [30], we know that β has much higher contribution to the thermal-induced OPD variation than α. Of course, contribution to the OPD variation cannot be the same depending on the amount of phase shift. Nevertheless, we can obviously say that the phase of the interference spectrum is shifted mainly with the modal index variation induced by the temperature change. On the other hands, n_{sur} does not affect the phase term because the guided modes are well confined inside the TMF and their evanescent fields seldom reach to the surrounding medium. However, n_{sur} is related to the amplitude of the output interference spectrum of Eq. (1). As a result, the temperature and the SRI can be determined separately by measuring the phase and the amplitude of the interference spectrum, respectively. In other words, the cross-sensitivity between the temperature and the RI measurements can be effectively eliminated by the proposed TMF probe.

Reading the signal variations of measurement factors can be efficiently processed by using the Fourier domain analysis. Assuming normal distribution of input spectrum and taking inverse Fourier-transform (IFFT) to Eq. (1), we obtain

$$I_{out}(z) = R^2(n_{sur})\cdot[\Gamma(z) + \frac{1}{2}\Gamma(z+\Delta z\,(T)) + \frac{1}{2}\Gamma(z-\Delta z\,(T))] \tag{4}$$

The first term is the autocorrelation peak that is related to the power spectrum of the light source itself. The last two terms are symmetric cross-correlation peaks that are related to the interference components. One thing to be pointed out is that n_{sur} varies with the temperature due to the thermo-optic effect, which should be considered when measuring the RIs of surrounding materials. Thus, variations of the liquid RI depending on its temperature can be quantified as TOC values by simply using the simultaneous sensing ability of the TMF probe.

Figure 3 are the measured spectra of the fabricated probes having TMF lengths of 10 mm (a) and 14 mm (b), respectively. A well-developed sinusoidal fringe pattern with an about 10 dB contrast was observed, which seemed to have a single frequency component dominantly.

#174874 - $15.00 USD Received 23 Aug 2012; revised 24 Sep 2012; accepted 24 Sep 2012; published 2 Oct 2012

Since the fringe spacing is inversely proportional to the TMF length, a longer TMF probe gives a faster varying interference signal.

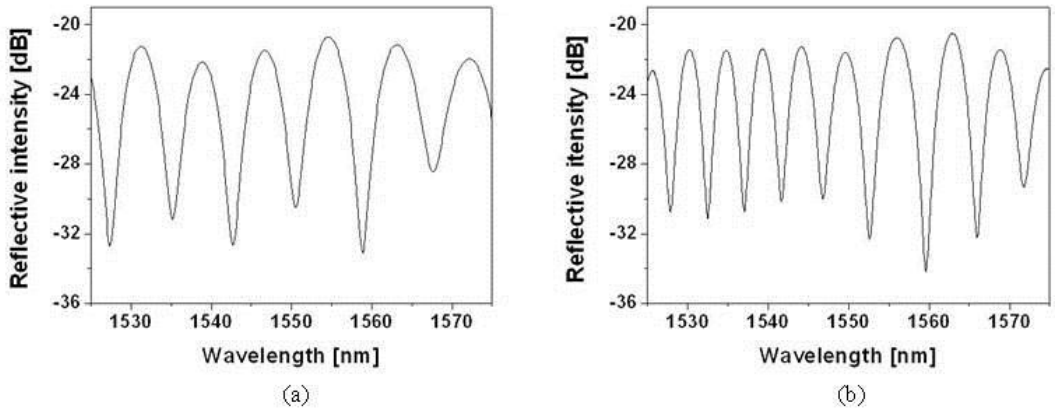

Fig. 3. Measured spectra of the fabricated interferometric probes having TMF lengths of (a) 10 mm and (b) 14 mm, respectively. Sinusoidal fringe patterns are well developed.

3. Simultaneous temperature and SRI sensing

For the temperature measurement, we put the probe into a temperature-controlled heating oven and slowly increased the temperature in order to ensure uniform thermal distribution. In this experiment, the surrounding medium was air, which was assumed to have a unit RI and to give about 4% Fresnel reflectance over the fibers. For the SRI measurement, the probe was immersed into certified RI liquids (Series: AAA, Cargille Laboratories Inc.) having the RI values from 1.300 to 1.395 with an interval of 0.005 and an accuracy of ± 0.0002. Since the RI data of liquids was provided at 589 nm, the calibrated RI data at 1550 nm was utilized. The spectrum variations were recorded by an optical spectrum analyzer (OSA) (86142B, Agilent Inc.). The probe utilized in experiments was the one having a TMF length of 14 mm. An amplified spontaneous emission (ASE) source (FLS-2300B, EXPO Inc., 1550 nm center wavelength, 50 nm bandwidth) was used as the input source. The wavelength resolution for the measurements was 0.06 nm, which was the maximum performance of the used OSA. Fig. 4(a) and 4(b) show the spectrum variations measured with the increasing temperature and SRIs, respectively. As increasing the temperature from 30 to 100 °C, the phase of interference signal was shifted; the fringe peaks were moved to the longer wavelength direction. Regardless of the substantial wavelength shift, Fig. 4(a) verifies that its intensity level was hardly ever changed with the temperature variation. We note that the air RI has an extremely low thermal dependency. On the other hands, Fig. 4(b) shows that both the DC level and the fringe contrast of the spectrum decreased with the increasing SRIs. However, any distinguishable phase shift was not observed in Fig. 4(b).

#174874 - $15.00 USD Received 23 Aug 2012; revised 24 Sep 2012; accepted 24 Sep 2012; published 2 Oct 2012

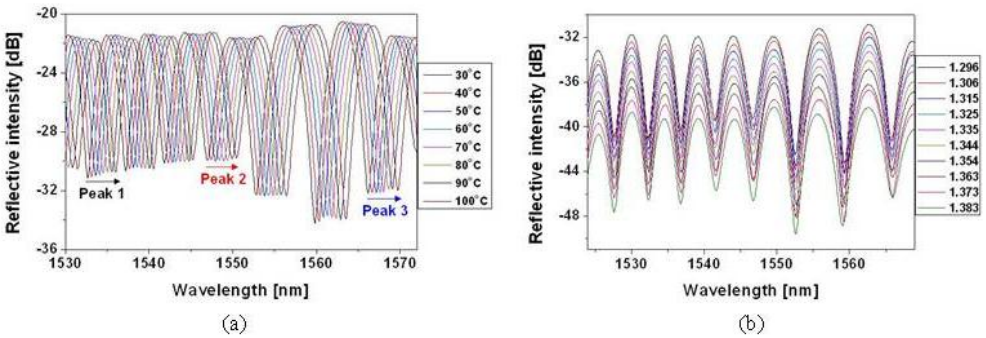

Fig. 4. Measured spectra with (a) temperature variations and (b) SRI variations. As increasing the temperature, the fringe peaks were shifted to the longer wavelength direction with almost no intensity change. With the SRI variations, on the other hands, both the DC level and the fringe contrast were reduced without macroscopic phase change.

In order to quantify the measured spectrum in a Fourier domain, we took IFFT to the wavelength spectra in Fig. 4 and got the Fourier spectra as Fig. 5. The left autocorrelation peak at zero frequency quantitatively corresponds to the DC level, while the right Fourier peak around 20/(100 nm) represents the interference component; its intensity and position stand for the fringe contrast and the OPD, respectively. As can be seen in Fig. 5(a) and its inset, there was almost no variation in the DC level with respect to the temperature but the right peak had a slight shift in position, which is caused by the thermally induced OPD variations. Figure 5(b) exhibits the Fourier spectrum variations responding to the SRIs. We observed that both peaks were reduced with the increasing SRIs. The intensity of the autocorrelation peak was higher than that of the signal peak. Also, the position of the autocorrelation peak was always fixed. Therefore, it was efficient to trace the amplitude of the autocorrelation peak for the quantitative measurement of SRIs. Standard deviation of the DC level in Fig. 5(a) was measured as ± 0.0026 and this value corresponds to an RI error of ± 0.0005. For the case of temperature measurements, tracing the fringe peak position in the spectral domain is better due to its higher visibility compared to the Fourier peak. However, measurements of phase shift in the spectral domain have a problem of 2π modular ambiguity so that the measurable temperature can be limited.

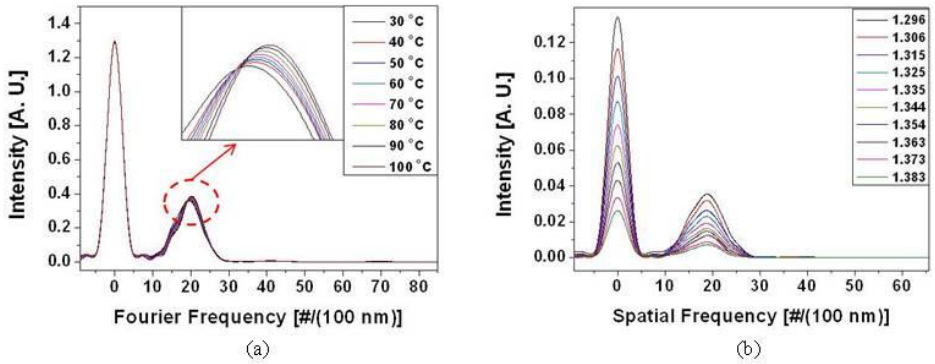

Fig. 5. (a) Fourier domain spectra obtained from inverse Fourier transform (IFFT) of Fig. 4(a) and (b) obtained from IFFT of Fig. 4(b). Intensity level was more quantitatively determined by IFFT compared to wavelength spectra.

With the signals measured in both spectral and Fourier domains, the quantitative signal variations with temperature and SRI were obtained. Figure 6(a) shows the tracing of the three peaks located at 1532, 1547, and 1566 nm in Fig. 4(a) in terms of temperature. It shows that

#174874 - $15.00 USD Received 23 Aug 2012; revised 24 Sep 2012; accepted 24 Sep 2012; published 2 Oct 2012

the peak wavelengths are almost linearly shifted with temperature. Also, we can see in the fitting curves of Fig. 6(a) that the peak located at the longer wavelength gives a slightly higher sensitivity to temperature than the other peaks. The wavelength-dependent sensitivity happens mainly due to the mode-dependent chromatic dispersion of the fiber. The average sensitivity was obtained to be 0.0494 nm/°C. Considering the wavelength resolution of 0.06 nm, an accuracy of temperature measurements was ± 1.21 °C. Figure 6(b) shows the measured intensity levels of the DC and the Fourier peaks responding to the SRI variations. The intensity behavior was well matched with a second order polynomial fitting curve since the amplitudes of a Fourier domain peak is proportional to the square of the amplitude reflection coefficient *R* in Eq. (4). Due to such independent responses to temperature and SRI, the simultaneous sensing of two parameters could be possible.

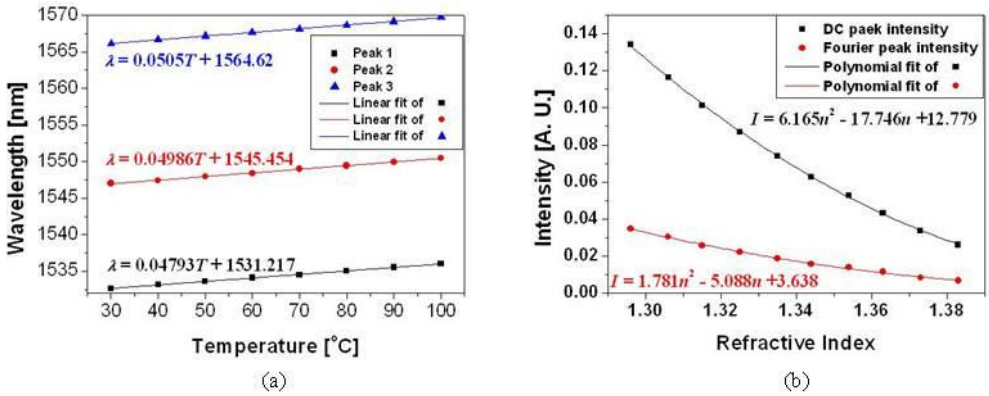

Fig. 6. (a) Wavelength response to the temperature and (b) Intensity variations of the DC and Fourier peak with respect to SRIs. Measured three peak wavelengths were almost linearly shifted with the increasing temperature while intensity variations were well fitted to polynomial curves.

4. Thermo-optic coefficient (TOC) measurement of liquid solutions

For a practical use of the proposed TMF probe, TOC measurements of liquid solutions have been performed [31]. The TOCs were acquired by dipping the fabricated probe into liquids and then measuring the reflection spectra at various liquid temperatures. Three beakers containing deionized water (DIW), ethanol, and acetone were prepared and put on a hot plate to increase the liquid temperature. Needle-type digital thermometer was kept near the TMF probe for temperature monitoring. The liquid temperature increased until just prior to the boiling point. It was expected that, with the increasing temperature, the peak wavelength was shifted as well as the intensity level was changed due to the thermal dependency of the liquid RIs.

#174874 - $15.00 USD Received 23 Aug 2012; revised 24 Sep 2012; accepted 24 Sep 2012; published 2 Oct 2012

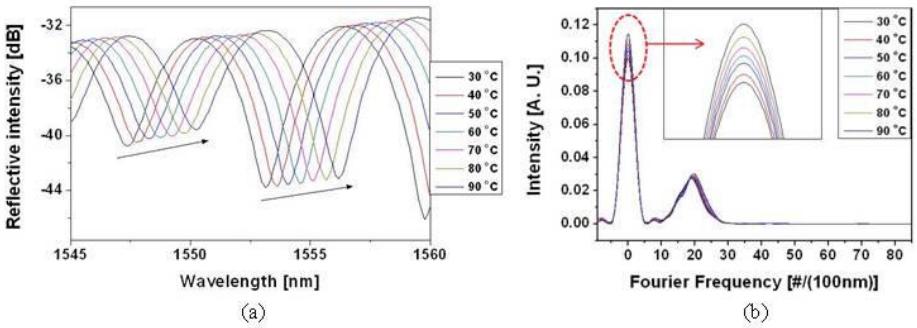

Fig. 7. (a) Variations in wavelength spectra with the increasing temperature of deionized water (DIW) and (b) their Fourier-transformed spectra. Peak wavelength was gradually shifted and at the same time intensity level was increased.

The measured spectra and their Fourier spectra for DIW are shown in Fig. 7(a) and 7(b), respectively. Variations in both the peak wavelength and the intensity level are obviously observed. The magnified inset of Fig. 7(b) verifies that the DC peak intensity increased with the increasing DIW temperature. By tracing the DC peak intensity and applying it to the relations measured in the previous section, we can get the thermal dependency of liquid RIs. Figure 8 shows the experimental results of the calculated RIs versus temperature for DIW (a), ethanol (b), and acetone (c). Since the density of liquids is inversely proportional to temperature, as well known, the liquid RIs were reduced as increasing their temperature. Acetone had the strongest thermal dependency among three liquid solutions. The obtained data points for DIW and ethanol were well fitted with 2nd order polynomial curves but acetone showed a linear tendency. In order to verify the experimental result, a previously reported formula, which is defined as an estimated equation based on various coefficients within the specified temperature, density, and wavelength [32], was used for a simulation curve plotted in Fig. 8(a) with a blue line. We can see that the experimental result has the similar reduction behavior with the simulated one although there exists a little deviation. It is thought that non-uniform thermal distribution of DIW might cause the deviation between the experimental and simulated result. Also, the simulation formula is validated within the wavelength range from 200 to 1100 nm [31], which means it can cause a little disagreement with the experimental result obtained around at 1550 nm.

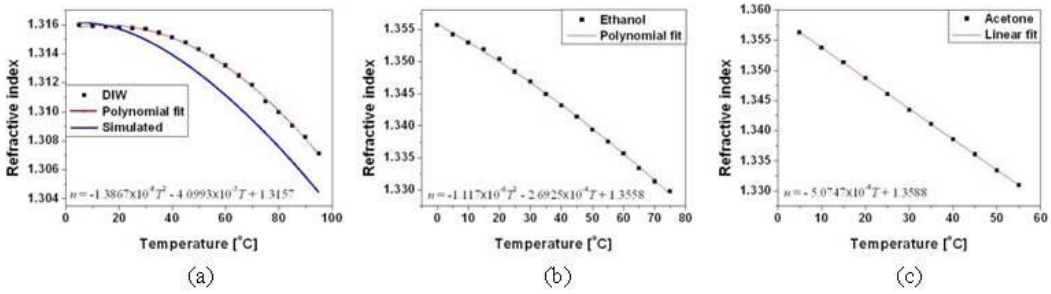

Fig. 8. Measured liquid RIs versus their temperature; (a) DIW, (b) ethanol, and (c) Acetone. RIs were reduced with the temperature and their dependencies were different to each other. Simulated relation for DIW is similar to the experimental result.

The TOCs of liquid solutions measured at a wavelength of 1550 nm are tabulated in Table 1, which was obtained by the derivative of fitting curves. The calculated TOC values of DIW and ethanol were obtained as a linear function of the temperature while acetone was constant with the temperature. As shown in Table 1, the reported TOCs of DIW, ethanol and acetone

#174874 - $15.00 USD Received 23 Aug 2012; revised 24 Sep 2012; accepted 24 Sep 2012; published 2 Oct 2012

were $-0.8\text{x}10^{-4}$, $-3.9\text{x}10^{-4}$ and $-5\text{x}10^{-4}$, respectively [33]. However, these data were obtained at a wavelength of 633 nm, which is quite different from our measurement done at 1550 nm. In spite of such a wavelength mismatch, our TOC measurements are not significantly different from the reported ones. Considering not enough data about liquid TOCs at 1550 nm, our results can be challenging as reference data.

Table 1. Measured Thermo-optic coefficients (TOCs) for three liquid solutions.

Liquid	Deionized water (DIW)	Ethanol	Acetone
TOC at 1550 nm [$^oC^{-1}$] (measured data)	$-2.7734\text{x}10^{-6}\cdot T - 4.0993\text{x}10^{-5}$	$-2.234\text{x}10^{-6}\cdot T - 2.6925\text{x}10^{-5}$	$-5.0747\text{x}10^{-4}$
TOC at 633 nm [$^oC^{-1}$] (reported data [31])	$-0.8\text{x}10^{-4}$	$-3.9\text{x}10^{-4}$	$-5\text{x}10^{-4}$

In order to confirm the spectral responses to temperature, the peak wavelength variations of liquid solutions are compared in Fig. 9. Almost similar slopes of them ensure that reading the peak wavelength is enough to be used as a temperature indicator. Thus, we can say that simple acquisition of liquid TOCs could be possible with the proposed TMF probe.

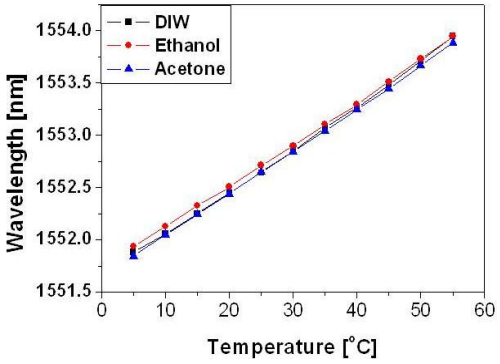

Fig. 9. Comparison of wavelength variations for three liquid solutions. They show almost similar slopes.

5. Conclusion and discussion

We have proposed and experimentally demonstrated a simple and compact TMF interferometric fiber sensor probe suitable for TOC measurements of liquid samples by characterizing the independent responses of the probe to temperature and SRI. Due to the unique waveguiding properties of the TMF, the fabricated probe allowed an in-line Michelson interferometer with LP_{01} and LP_{02} modes. Most of the in-line fiber interferometers usually face a mode uncertainty problem, which causes complex mutual modal interferences. Also, since each mode has different sensitivity to external variations, the mode uncertainty can adversely affect the sensing performance. However, the proposed TMF probe involves only specified modal interference component in the measured signal, so that more stable and accurate sensing is possible without complex modal analysis. Further, the simple probe structure, involving only one fusion-splicing without other complicated processes, can make the sensor to be firm, stable and easy for packaging.

Through the experiments, it has been revealed that the proposed probe has an effective structure for measuring temperature and SRI at the same time because the response to each perturbation was independent. The peak position of an interference Fourier spectrum could be used for indicating the temperature while the intensity level could be used for the SRI value. The relations between measurands and signal values were quantitatively obtained with the help of the Fourier domain analysis. As a practical application for investigating the thermo-optic effect of liquid solutions, we have experimentally tried to measure the TOCs of several liquid solutions including DIW, ethanol, and acetone at 1550 nm by using the simultaneous

#174874 - $15.00 USD Received 23 Aug 2012; revised 24 Sep 2012; accepted 24 Sep 2012; published 2 Oct 2012

sensing ability of the TMF probe. The measured TOC values were obtained as $-2.7734\text{x}10^{-6}\cdot T$ $-4.0993\text{x}10^{-5}$ for DIW, $-2.234\text{x}10^{-6}\cdot T$ - $2.6925\text{x}10^{-4}$ for ethanol, and $-5.0747\text{x}10^{-4}$ for acetone. It is expected that the proposed TMF probe can be widely applied for fields of studying biomedical and biochemical solutions.

Acknowledgments

This work was supported in part by Basic Science Research Program through the National Research Foundation of Korea (NRF) funded by the Ministry of Education, Science and Technology (No. R15-2008-006-02002-0) and in part by a grant from the institute of Medical System Engineering (iMSE) in the GIST. Korea.

#174874 - $15.00 USD Received 23 Aug 2012; revised 24 Sep 2012; accepted 24 Sep 2012; published 2 Oct 2012